Stem Cell Research 17 (2016) 266–272

Contents lists available at ScienceDirect

Stem Cell Research

journal homepage: www.elsevier.com/locate/scr

Lab Resource: Stem Cell Line

Murine transgenic iPS cell line for monitoring and selection of cardiomyocytes

Azra Fatima, Guoxing Xu, Filomain Nguemo, Alexey Kuzmenkin [1], Karsten Burkert, Jürgen Hescheler, Tomo Šarić *

Center for Physiology and Pathophysiology, Institute for Neurophysiology, Medical Faculty, University of Cologne, Cologne, Germany

ARTICLE INFO

Article history:
Received 1 January 2016
Received in revised form 20 June 2016
Accepted 19 July 2016
Available online 21 July 2016

ABSTRACT

We report here a transgenic murine induced pluripotent stem cell (iPSC) line expressing puromycin *N*-acetyltransferase (PAC) and enhanced green fluorescent protein (EGFP) under the control of α-myosin heavy chain promoter. This transgenic cell line reproducibly differentiates into EGFP-expressing cardiomyocytes (CMs) which can be generated at high purity with puromycin treatment and exhibit molecular and functional properties of immature heart muscle cells. This genetically modified iPSC line can be used for assessment of the utility of CMs for myocardial repair, pharmacological and toxicological applications and development of improved cardiac differentiation protocols.

Resource table.

Name of stem cell line	αPIG-AT25-miPSC
Institution	Center for Physiology and Pathophysiology, Institute for Neurophysiology, Medical Faculty, University of Cologne, Cologne, Germany
Person who created resource	Azra Fatima
Contact person and email	Tomo Saric, tomo.saric@uni-koeln.de
Date archived/stock date	8 September 2012
Origin	Murine iPS cell line TiB7.4 generated with retrovirally encoded OSKM reprogramming factors (kindly provided by Rudolf Jaenisch and Alexander Meissner)
Type of resource	Genetically modified murine iPS cell line for generation of CMs
Sub-type	Cell line
Transgenes	SV40 promoter-driven amino 3-glycosyl phosphotransferase (neo) gene; α-myosin heavy chain promoter-driven puromycin *N*-acetyltransferase (PAC) and enhanced green fluorescent protein (EGFP) genes
Authentication	Resistance of transgenic iPSC line to neomycin; sensitivity of non-CMs to puromycin; expression of EGFP protein and PAC transcripts in purified CMs
Link to related literature	http://www.ncbi.nlm.nih.gov/pubmed/24042016 http://www.ncbi.nlm.nih.gov/pubmed/25022569 http://www.ncbi.nlm.nih.gov/pubmed/24219308 http://www.ncbi.nlm.nih.gov/pubmed/26021268 http://www.ncbi.nlm.nih.gov/pubmed/25900017

Resource details

Large amounts of highly pure and functionally intact cardiomyocytes (CMs) are required for applications in tissue engineering, drug discovery and toxicity testing. The most efficient system for production of pure CMs at large quantities is in suspension mass cultures (Hemmi et al., 2014; Kempf et al., 2014; Nguyen et al., 2014; Schroeder et al., 2005) and relies on regulated expression of exogenous reporter and/or selection markers under the control of a cardiospecific promoter (Anderson et al., 2007; Friedrichs et al., 2015; Kita-Matsuo et al., 2009; Klug et al., 1996; Kolossov et al., 2006; Ritner et al., 2011; van Laake et al., 2010). Here, we have genetically modified murine induced

* Corresponding author.
E-mail address: tomo.saric@uni-koeln.de (T. Šarić).
[1] Bayer Business Services GmbH, Leverkusen, Germany.

http://dx.doi.org/10.1016/j.scr.2016.07.007

pluripotent stem cell (miPSC) line TiB7.4 (Meissner et al., 2007) to obtain the transgenic line αPIG-AT25 by transfecting the cells with the plasmid expressing puromycin *N*-acetyltransferase (PAC) and enhanced green fluorescent protein (EGFP) under the control of the CM-specific α-myosin heavy chain (α-MHC) promoter (Fig. 1A). The αPIG-AT25 miPSCs exhibit pluripotent stem cell colony morphology (Fig. 1B) and express alkaline phosphatase (Fig. 1C), the self-renewal protein Oct4 (Fig. 1D) and pluripotent stem cell marker SSEA1 (Fig. 1E). The promoter regions of *Nanog* and *Oct4* genes are similarly hypomethylated in αPIG-AT25 iPSCs and transgenic murine embryonic stem cells (ESC) line αPIG44 that was generated previously using the same vector (Kolossov et al., 2006) (Fig. 1F). In contrast, the same promoter regions were highly methylated in tail tip fibroblasts (TTF), from which the iPSCs were generated, and in αPIG-AT25 miPSC-derived CMs (Fig. 1F).

The transgenic iPSCs differentiate into embryoid bodies (EBs) containing spontaneously beating EGFP-positive areas, which first appear on day 7–9 of differentiation (Fig. 2A). After 7 days of puromycin treatment, nearly all non-cardiomyocytes in EBs are eliminated and the resistant cells survive as spontaneously beating EGFP-positive clusters (Fig. 2A). Flow cytometric analyses of clusters dissociated into single cells revealed that these clusters are enriched in CMs up to 97% (Fig. 2C) and that all EGFP-positive cells are uniformly stained for cardiac troponin T (cTnT) (Fig. 2D). When plated on fibronectin-coated plates, these CMs grow as a monolayer of spontaneously contracting CMs (Fig. 2B) which express cardiac proteins troponin T, α-MHC and α-actinin (Fig. 2E) and exhibit immature cross-striation pattern (Fig. 2F). Semi-quantitative RT-PCR analyses showed that cardiac transcripts *Mef2c*, *GATA4*, *NKx2.5*, *TnnC*, *TnnT* and *RyR2* as well as transgenic *PAC* are enriched in αPIG-AT25-iPSC- and αPIG44-ESC-derived CMs compared to undifferentiated cells and intact EBs (Fig. 3A). In contrast, the transcripts for mesodermal (ε-globin) and endodermal markers α-fetoprotein (*Afp*), *Sox17* and *CD31* were not detected (Fig. 3A). As expected, virally encoded transcripts were not detectable in ESCs. However, they are expressed at low levels in undifferentiated iPSCs and iPSC-derived EBs but not in purified iPSC-derived CMs with the exception of retrovirally encoded *Oct4* that appears to be incompletely silenced in CMs (Fig. 3B). Quantitative RT-PCR analyses also demonstrated that CMs are highly enriched in transcripts encoding for transcription factor *Nkx2.5* and structural proteins cardiac ventricular myosin light chain 2 (*Myl2*) and α heavy chain subunit of cardiac myosin (*Myh6*) as well as in transcripts encoding for the vector-derived EGFP (Fig. 3C). These analyses also show that CMs express no or very low levels of pluripotency-associated transcripts for *Nanog* and *Oct4* as well as endoderm-specific mRNAs for *Afp* and *Sox17* (Fig. 3C).

Action potentials (APs) of spontaneously beating αPIG-AT25-iPSC-derived CMs exhibit a variety of morphologies, including pacemaker-like, atrial-like, and ventricular-like APs (Fig. 4A). However, most APs could not be further specified. The whole-cell current-clamp measurements revealed the existence of intact β-adrenergic and muscarinic signalling cascades in lineage-selected CMs as demonstrated by the response to β-adrenergic receptor agonist isoproterenol (Iso) and muscarinic receptor agonist carbachol (CCh), which was similar to that of previously reported murine iPSC-derived CMs (Fig. 4B–D) (Kuzmenkin et al., 2009; Nembo et al., 2015; Pfannkuche et al., 2009). Purified iPSC-derived CMs expressed functional voltage-gated Na^+-, L-type Ca^{2+}- and K^+-channels with current densities that were comparable to that of iPSC-derived CMs reported previously (Kuzmenkin et al., 2009) (Fig. 5A–D). The contribution of different K^+-channels to the net depolarization-activated outward K^+-current was similar in drug-selected iPSC- and ESC-derived CMs. The current-voltage relationships of all currents were also indistinguishable between iPSC- and ESC-derived CMs (Fig. 5E).

Materials and methods

iPSC culture

This miPSC line was maintained on irradiated mouse embryonic fibroblasts (MEF) in Dulbecco's Modified Eagle's Medium (Gibco) supplemented with 15% fetal bovine serum (FBS), 1× non essential amino acids, 2 mM L-glutamine, 50 μM 2-mercaptoethanol, and 1000 U/ml Leukemia Inhibitory Factor (LIF; ESGRO, Chemicon International). The cells were passaged regularly at 2–3 day interval by 0.05% trypsin/EDTA dissociation.

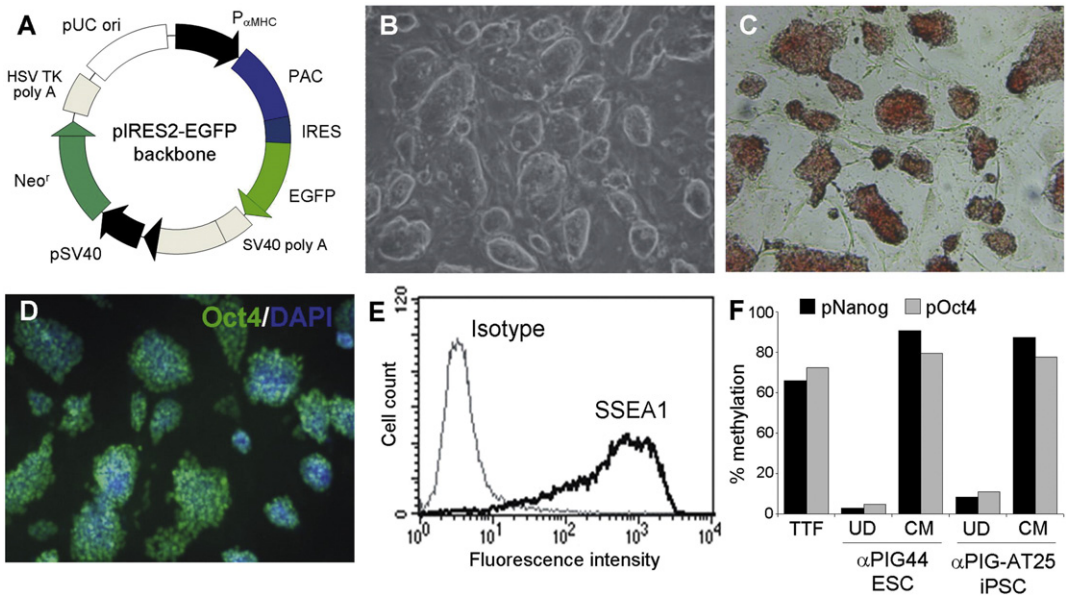

Fig. 1. Generation and characterization of transgenic murine αPiG-AT25 iPSC line. A. The map of the α-MHC–PAC–IRES–EGFP (αPIG) vector used for genetic modification of iPSCs. In this vector, the α-myosin heavy chain (α-MHC) promoter drives the expression of puromycin *N*-acetyltransferase (PAC) and the IRES-flanked enhanced green fluorescent protein (EGFP). The plasmid also encodes for a neomycin resistance (neo^r) gene amino 3-glycosyl phosphotransferase which is controlled by a constitutive SV40 promoter. B. Phase contrast images of undifferentiated iPSCs growing on irradiated MEFs. C. Alkaline phosphate staining of iPSC colonies. D. Detection of Oct4 expression by immunocytochemistry. Nuclei were counterstained with Hoechst 33,342. E. Flow cytometric analysis of SSEA1 expression on undifferentiated iPSCs. F. Methylation status of *Oct4* and *Nanog* promoters in tail tip fibroblasts (TTF) used for generation of iPSCs, undifferentiated (UD) transgenic αPiG-AT25 iPSCs and αPiG44 ESCs and in puromycin-selected CMs derived from them.

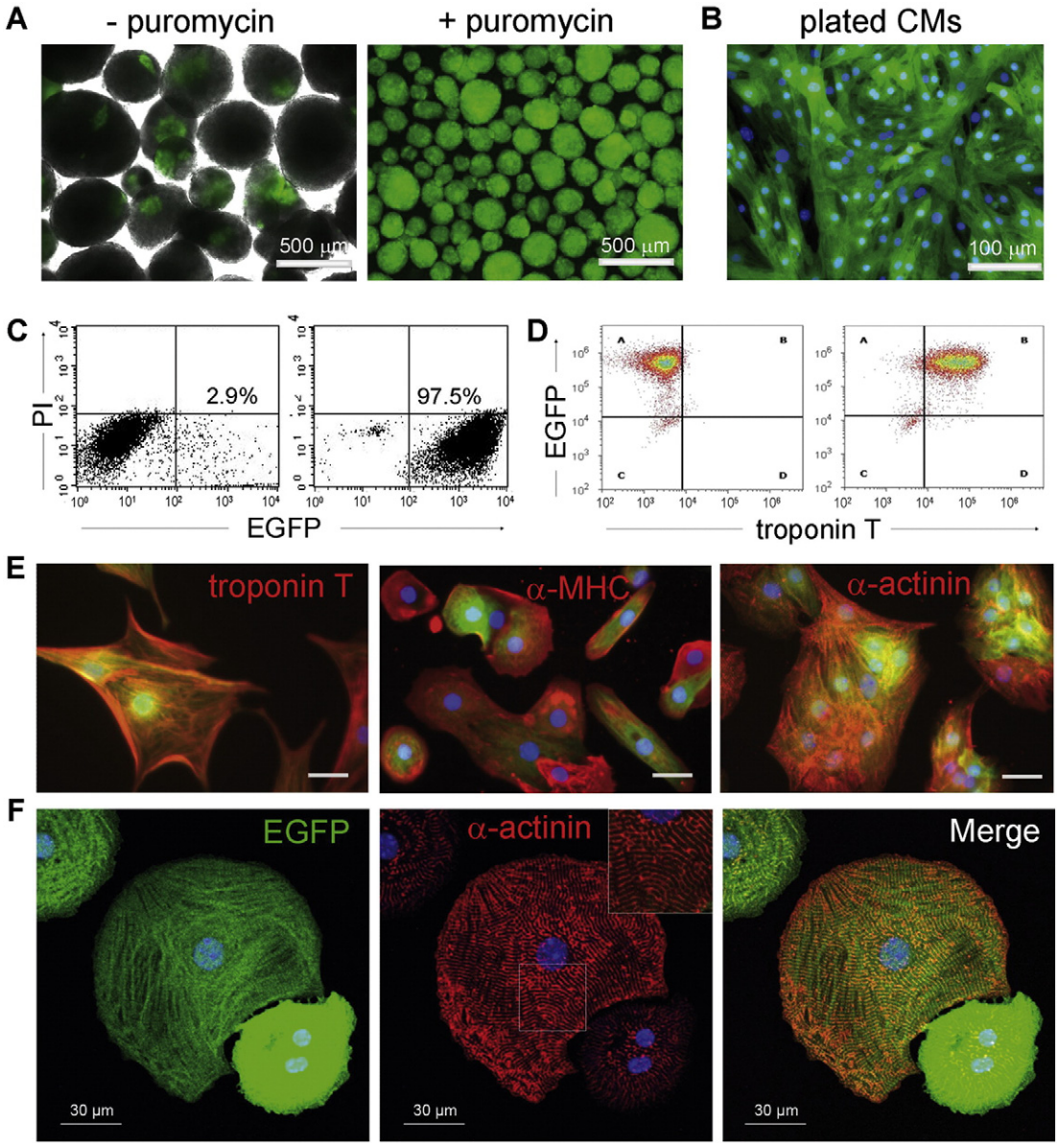

Fig. 2. Generation of CMs from transgenic iPSCs by puromycin selection. Intact αPiG-AT25 iPSC-derived EBs at day 9 of differentiation without exposure to puromycin exhibiting EGFP-positive areas (left panel). Pure cardiac clusters obtained after 7 days of puromycin treatment are shown in the right (EGFP-channel) panel. B. Enzymatically dissociated drug-selected CMs grow as a monolayer of EGFP-positive cells on fibronectin-coated tissue culture plates. C. Flow cytometric analysis of the frequency of EGFP-positive CMs in dissociated cardiac clusters at day 16 of differentiation without (left panel) and with (right panel) puromycin treatment for seven days. D. Flow cytometry reveals co-expression of cardiac troponin T with EGFP in puromycin selected CMs stained with isotype control antibody (left panel) and anti-troponin T (right panel). E. Immunocytochemical stainings of plated transgenic iPSC-derived CMs with anti-troponin T, anti-α-MHC and anti-sarcomeric α-actinin. Scale bars: 50 μm. F. Confocal fluorescence microscopy of purified αPiG-AT25 iPSC-derived CMs at large magnification indicates cell morphology and sarcomeric structures resembling immature CMs. Nuclei in panels B, E and F were counterstained with Hoechst 33342.

Genetic modification of iPSCs

The α-MHC–PAC–IRES–EGFP (αPIG) vector (Fig. 1A) was linearized by *Sac*I and 5×10^6 cells were electroporated with 14 μg of this construct in Gene Pulser cuvette (0.4 cm electrode, gap 50, BioRad) at 260 V and 500 μF. After neomycin selection, resistant clones were isolated and propagated. The AT25 clone was selected based on its high CM differentiation efficiency.

Differentiation to CMs

iPSCs were differentiated in a spinner flask system. Briefly, 1×10^6 undifferentiated cells were suspended in 14 ml of differentiation medium (Iscove's Modified Dulbecco's Medium supplemented with 20% FBS, 10 μM β-Mercaptoethanol and 1× non-essential amino acids) and cultured for 2 days in non-adherent plates on a shaker under continuous agitation to allow formation of EBs. At day 2 of differentiation, the EBs were counted and diluted into fresh 200 ml medium to a density of 28,000 EBs per spinner flask (Cellspin 250, Integra Biosciences). The differentiation process continued for 6–7 days without medium change until the first appearance of green fluorescence in spontaneously beating EBs. On day 9 of differentiation, fresh medium supplemented with puromycin (8 μg/ml) was added to purify CMs. After 2–3 days of selection, the surviving cardiac clusters were pooled and further incubated for another 5–6 days on the shaker in fresh medium with puromycin in non-adherent culture dishes. Fresh medium containing puromycin was replaced every 2 days until pure beating cardiac clusters were obtained on day 16 of differentiation after 7 days of puromycin treatment.

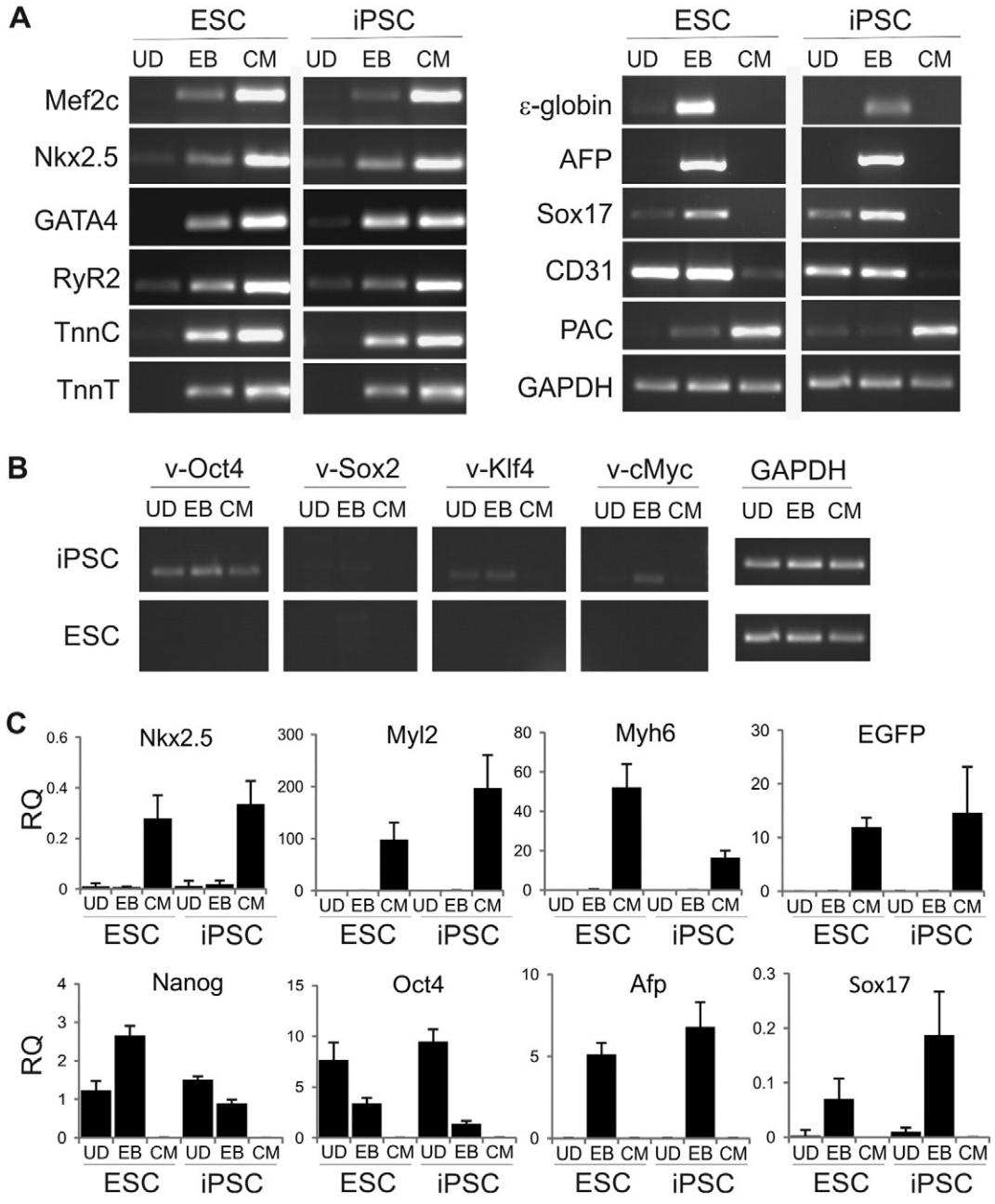

Fig. 3. Expression of cardiac- but not lineage-specific genes and incomplete silencing of viral *Oct4* transgene in αPiG-AT25 iPSC-derived CMs. A. RT-PCR analysis of indicated cardiac (left panel) and non-cardiac transcripts (right panel) in undifferentiated cells (UD), day 16 EBs and purified day 16 CMs derived from αPIG44-ESCs or αPiG-AT25-iPSCs. B. RT-PCR analysis of virally-encoded reprogramming factors in αPIG44-ESCs and αPiG-AT25-iPSCs, their EB counterparts and pure CMs. C. Quantitative real-time PCR analysis of indicated transcripts in undifferentiated (UD) cells, day 16 EBs and day 16 CMs derived from αPIG44-ESCs or αPiG-AT25-iPSCs.

RT-PCR

Total RNA was isolated from undifferentiated iPSCs and ESCs, day 16 EBs and day 16 CMs using TRIzol (Invitrogen). DNase I-pretreated RNA was reverse-transcribed by Superscript II RTase (Invitrogen) using random hexamers for priming. The cDNA was amplified using JumpStart Red Taq PCR-Ready Mix (Sigma) and the resulting products analyzed by agarose gel electrophoresis.

Immunocytochemistry

Single CMs were plated on fibronectin-coated μ-dishes (Ibidi) at 0.3×10^6 cells/plate in differentiation medium containing 8 μg/ml puromycin. After 2–3 days adherent CMs were fixed in 4% buffered paraformaldehyde (pH 7.5), permeabilized by Triton X-100 and stained with α-actinin (clone EA-53, 1:400; Sigma), cardiac troponin T (1:200, Cat. No. sc20025, Santa Cruz) and αMHC (clone A4.1025, 1:100, Sigma) antibodies. Secondary antibodies were conjugated to AlexaFluor-555 or AlexaFluor-647 (1:1000, Invitrogen). Nuclei were stained with Hoechst 33,342 (1:5000, Invitrogen) and samples were examined using an Axiovert 200 M florescence microscope (Zeiss).

Flow cytometry

CMs were prepared by dissociation with 0.05% Trypsin/EDTA. Cell clumps were removed by passing through the cell strainer, and cells were analyzed by flow cytometry (FACScan, BD Pharmingen). Propidium iodide was used for dead cell staining. For intracellular

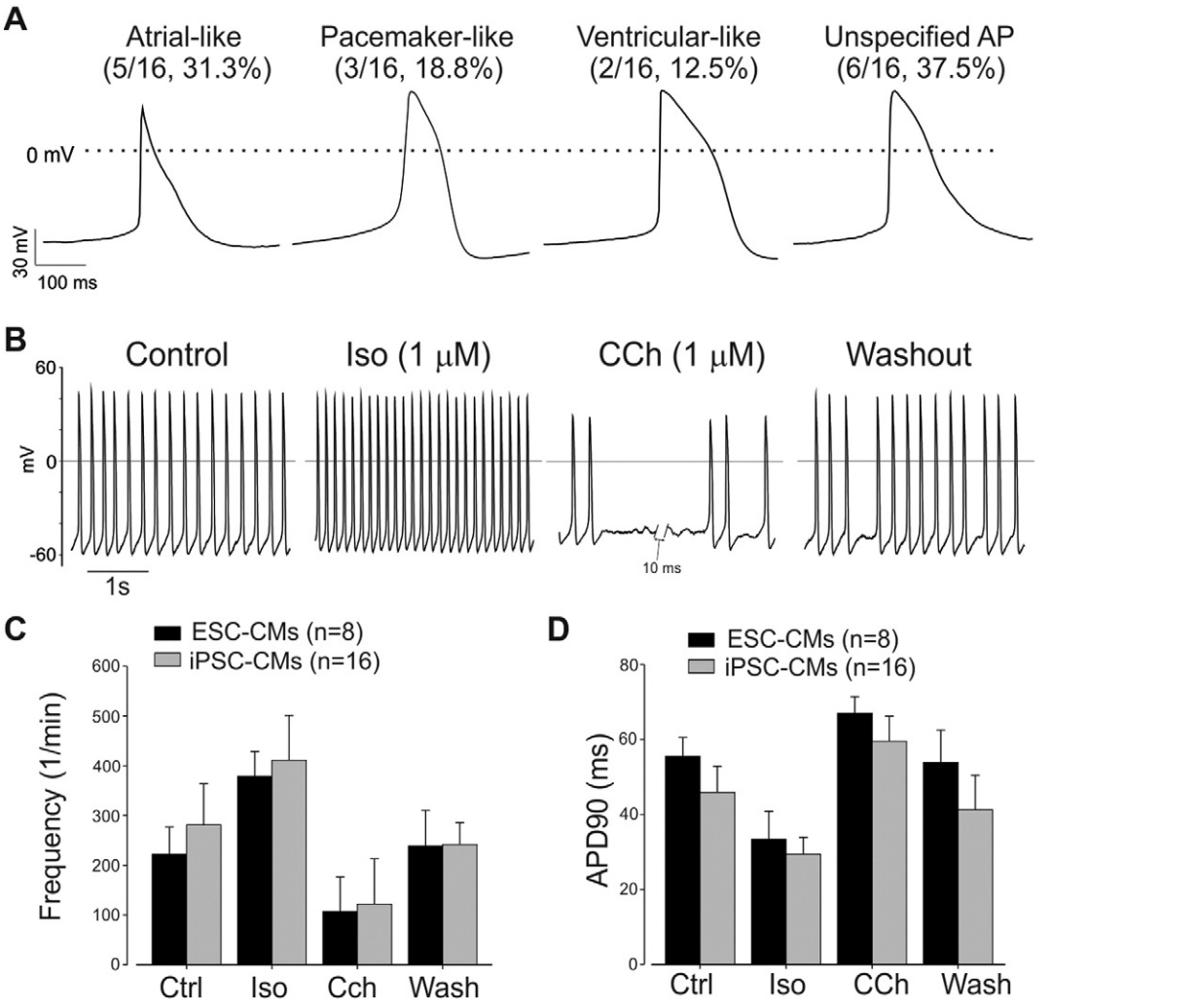

Fig. 4. Current-clamp characterization of murine αPiG-AT25 iPSC-derived CMs. A. The atrial-like, pacemaker-like and ventricular-like AP traces of single iPSC-derived CMs. 6 out of 16 measured APs (37.5%) could not be definitively categorized. B. Representative AP recording traces showing the effect of isoproterenol (Iso, 1 μM) and carbachol (CCh, 1 μM) on drug selected iPSC-CMs. Comparison of the effect of Iso and CCh on the spontaneous AP frequency (C) and the AP duration at 90% repolarization (APD90) (D) in αPiG-AT25-iPSC- and αPiG44-ESC-derived CMs.

staining with cTnT antibodies, cells were fixed and later permeabilized with 1% saponin (Sigma-Aldrich) in 5% BSA diluted in PBS for 1 h at room temperature before incubating with 1:50 diluted monoclonal murine anti-cTnT antibody in 1% Saponin and 0.8% BSA in PBS for 30 min at 4 °C. The secondary anti-mouse antibody (Alexa-Fluor 555 labeled, Molecular Probes) was diluted 1:100 in 1% Saponin and 0.8% BSA in PBS and incubated for 1 h at 4 °C.

Electrophysiology

For patch-clamp experiments, puromycin-purified cardiac clusters were dissociated into single CMs by using collagenase B on day 14 of differentiation and then plated on 0.1% gelatin-coated 22 × 22 mm square glass cover slips in 3.5 cm dishes. Cells were incubated for 24–48 h before measurements were performed. Individual CMs were selected according to their typical morphology and spontaneous beating activity. The glass cover slips containing the cells were placed into a temperature-controlled (37 °C) recording chamber and perfused continuously with extracellular solution. Cell membrane capacitance was determined on-line using the Pulse program (Heka Elektronik). APs of spontaneously beating CMs were recorded by the whole-cell current-clamp technique using an EPC-9 amplifier and operated through the PULSE acquisition software (HEKA Elektronik, Lambrecht, Germany). Response of CMs to hormonal regulation was assessed by administering isoproterenol (Iso) and carbachol (CCh) (Sigma-Aldrich). The standard whole-cell patch-clamp recording technique (Hamill et al., 1981) in the voltage-clamp mode was used for recording voltage-gated Na^+-, L-type Ca^{2+}-, and depolarization-activated outward K^+-channel currents.

For recording Na^+ and L-type Ca^{2+} currents, extracellular solution contained (in mM): NaCl 120, KCl 5, $CaCl_2$ 3.6, $MgCl_2$ 1, tetraethylammonium (TEA) chloride 20, HEPES 10, pH adjusted to 7.40 at 37 °C with TEA-OH. For recording K^+ currents, extra cellular solution contained (in mM): *N*-methyl-D-glucamine (NMG) chloride 135, KCl 5, $CaCl_2$ 3.6, $MgCl_2$ 1, $NiCl_2$ 3, HEPES 10, pH adjusted to 7.40 at 37 °C with NMG. Intracellular solutions contained: for Na^+ and Ca^{2+} currents (in mM) – CsCl 120, $MgCl_2$ 3, MgATP 5, EGTA 10, HEPES 5, pH adjusted to 7.40 with CsOH; and for K^+ current recordings (in mM) – KCl 50, K-aspartate 80, $MgCl_2$ 1, MgATP 3, EGTA 10, HEPES 10, pH adjusted to 7.40 with NMG. If not stated otherwise, all reagents were obtained from Sigma-Aldrich Chemie GmbH, Germany.

Na^+ channel currents were elicited by a family of 100-ms depolarizations from a − 90 mV holding potential (HP) to voltages ranging from −60 to +55 mV in 5-mV steps. Ca^{2+} channel currents were measured with a double-pulse protocol. First, a 100-ms depolarization from a HP of −90 mV to −40 mV was applied to inactivate Na^+ and T-type

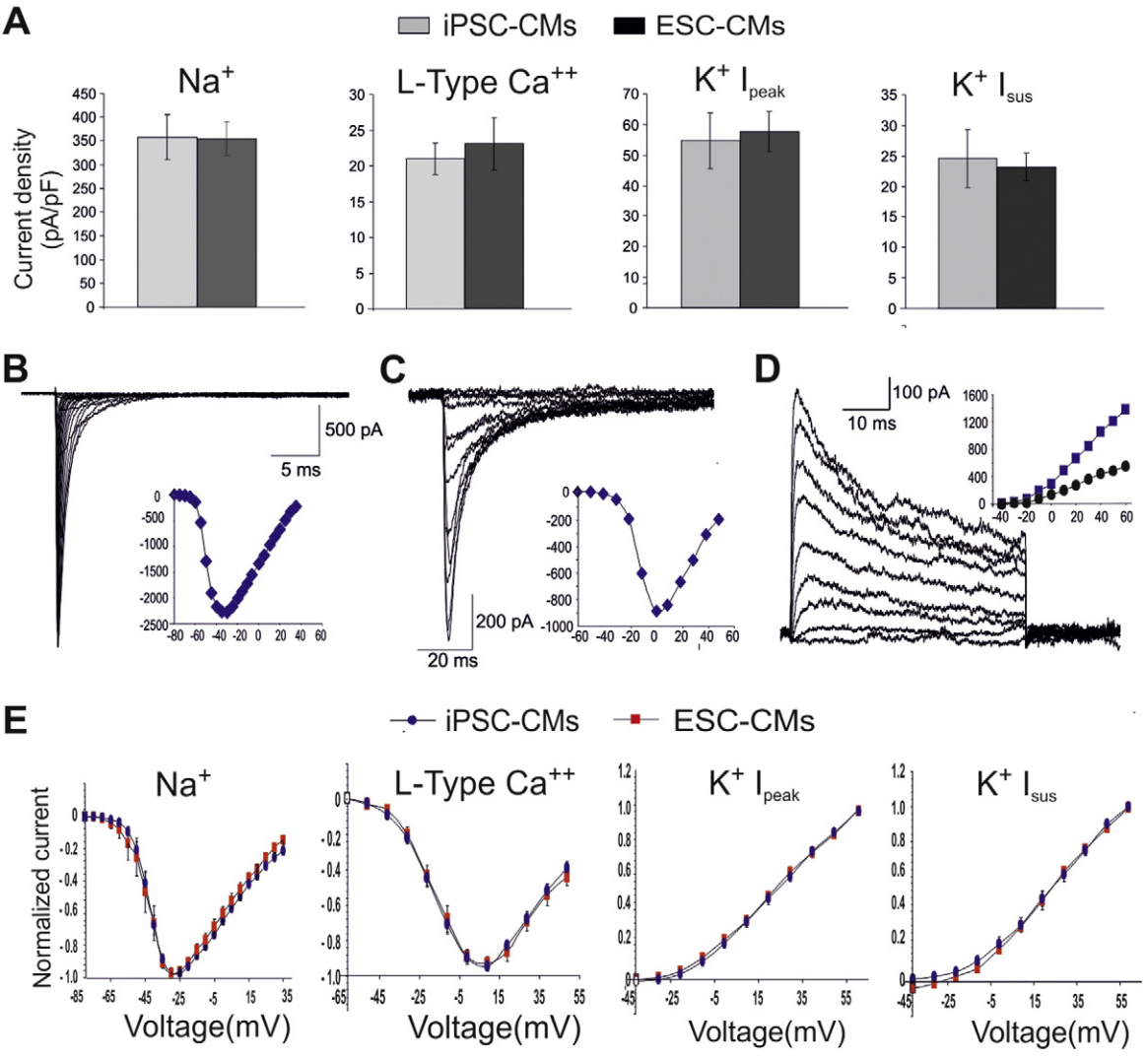

Fig. 5. Functional voltage-gated ion channels in iPSC-derived CMs. A. Current densities of Na^+, L-type Ca^{2+} and different depolarization-activated outward K^+ channels (fast activating currents, comprising I_{peak}, and slow activating currents remaining at the end of depolarization, comprising I_{sus}) were determined in αPiG-AT25-iPSC- and αPiG44-ESC-derived CMs using the whole-cell voltage-clamp. B. Na^+ channel currents in iPSC-derived CMs were elicited by a family of 100-ms depolarizations from a −90 mV holding potential (HP) to voltages ranging from −60 to +55 mV in 5-mV steps. C. Ca^{2+} channel currents in iPSC-derived CMs were measured with a double-pulse protocol. First, a 100-ms depolarization from a HP of −90 mV to −40 mV was applied to inactivate Na^+ and T-type Ca^{2+} channels, then L-type Ca^{2+} channels were elicited by a family of 67-ms depolarizations to voltages ranging from −60 to +50 mV in 10-mV steps. In Na^+ and Ca^{2+} channel experiments, leak subtraction -P/4 protocol was applied from HP of −90 mV. D. Depolarization-activated outward K^+ currents in iPSC-derived CMs were elicited by a family of 500-ms depolarizations from a −80 mV HP to voltages ranging from −40 mV to +60 mV in 10 mV steps. We analyzed peak current values (I_{peak}) and sustained currents (I_{sus}, remaining currents at the end of depolarization). Leak and capacity transients were eliminated by 4 pulses P/10 from a −80 mV HP. In figure inlays in panels B-D amplitudes of a corresponding current normalized to a cell size (current density values, in pA/pF) are plotted against test voltages (in mV). In panel D, squares represent I_{peak} and circles represent I_{sus} density values. E. Current-voltage relationships of Na^+, L-type Ca^{2+}, I_{peak}, and I_{sus} currents in puromycin selected iPS- and ES-CMs. Current amplitudes are normalized to a maximum and are plotted against test voltages (in mV). The number of cells used in voltage-clamp experiments range from n = 15 to n = 43. None of the values were statistically significantly different between transgenic iPSC- and ESC-derived CMs.

Ca^{2+} channels, then L-type Ca^{2+} channels were elicited by a family of 67-ms depolarizations to voltages ranging from −60 to +50 mV in 10-mV steps. In Na^+ and Ca^{2+} channel experiments, leak subtraction -P/4 protocol was applied from HP of −90 mV. Depolarization-activated outward K^+ currents were elicited by a family of 500-ms depolarizations from a − 80 mV HP to voltages ranging from −40 mV to +60 mV in 10 mV steps. We analyzed peak current values (I_{peak}) and sustained currents (I_{sus}, remaining currents at the end of depolarization). Leak and capacity transients were eliminated by 4 pulses P/10 from a −80 mV HP.

The data on L-type Ca^{2+} currents and Na^+ currents was collected simultaneously. There was no contamination of L-type Ca^{2+} currents with Na^+, as those were fully inactivated with a long conditioning pre-pulse to −40 mV, before L-type Ca^{2+} currents were elicited by a test pulse. L-type currents were also always checked for the presence of fast activation component suggesting a contamination with Na^+ current, but there was no such component visible. L-type Ca^{2+} channels were not affected by the pre-pulse, as they activate in a more positive voltage range. Additionally, the Ca^{2+} current contamination in Na^+ currents was also estimated. As L-type currents were always co-measured in the cells where Na^+ channel currents were recorded, we compared the amplitudes. If the maxima at corresponding potentials are compared, the mean contamination of Na^+ currents with an L-type current is <1%, in the most relevant voltage range (from −50 to −10 mV) it is <0.5%. Considering that the activation of L-type Ca^{2+} channels is 5–10 times slower than the Na^+ channel activation, we estimate the L-type current contribution to <0.1%. Thus, the tiny Ca^{2+} current contamination in the Na^+ currents could be neglected.

Data are presented as the mean ± standard error of the mean (SEM). Student's *t*-test was applied for statistical evaluation.

Acknowledgements

This study was supported by the grants from the Federal Ministry for Education and Research (BMBF, grant No. 01GN0947) and Köln-Fortune Program.

References

Anderson, D., Self, T., Mellor, I.R., Goh, G., Hill, S.J., Denning, C., 2007. Transgenic enrichment of cardiomyocytes from human embryonic stem cells. Mol. Ther. 15, 2027–2036.

Friedrichs, S., Malan, D., Voss, Y., Sasse, P., 2015. Scalable electrophysiological investigation of iPS cell-derived cardiomyocytes obtained by a lentiviral purification strategy. J. Clin. Med. 4, 102–123.

Hamill, O.P., Marty, A., Neher, E., Sakmann, B., Sigworth, F.J., 1981. Improved patch-clamp techniques for high-resolution current recording from cells and cell-free membrane patches. Pflugers Arch. 391, 85–100.

Hemmi, N., Tohyama, S., Nakajima, K., Kanazawa, H., Suzuki, T., Hattori, F., Seki, T., Kishino, Y., Hirano, A., Okada, M., Tabei, R., Ohno, R., Fujita, C., Haruna, T., Yuasa, S., Sano, M., Fujita, J., Fukuda, K., 2014. A massive suspension culture system with metabolic purification for human pluripotent stem cell-derived cardiomyocytes. Stem Cells Transl. Med. 3, 1473–1483.

Kempf, H., Olmer, R., Kropp, C., Rückert, M., Jara-Avaca, M., Robles-Diaz, D., Franke, A., Elliott, D.A., Wojciechowski, D., Fischer, M., Roa Lara, A., Kensah, G., Gruh, I., Haverich, A., Martin, U., Zweigerdt, R., 2014. Controlling expansion and cardiomyogenic differentiation of human pluripotent stem cells in scalable suspension culture. Stem Cell Rep. 3, 1132–1146.

Kita-Matsuo, H., Barcova, M., Prigozhina, N., Salomonis, N., Wei, K., Jacot, J.G., Nelson, B., Spiering, S., Haverslag, R., Kim, C., Talantova, M., Bajpai, R., Calzolari, D., Terskikh, A., McCulloch, A.D., Price, J.H., Conklin, B.R., Chen, H.S., Mercola, M., 2009. Lentiviral vectors and protocols for creation of stable hESC lines for fluorescent tracking and drug resistance selection of cardiomyocytes. PLoS One 4, e5046.

Klug, M.G., Soonpaa, M.H., Koh, G.Y., Field, L.J., 1996. Genetically selected cardiomyocytes from differentiating embronic stem cells form stable intracardiac grafts. J. Clin. Invest. 98, 216–224.

Kolossov, E., Bostani, T., Roell, W., Breitbach, M., Pillekamp, F., Nygren, J.M., Sasse, P., Rubenchik, O., Fries, J.W., Wenzel, D., Geisen, C., Xia, Y., Lu, Z., Duan, Y., Kettenhofen, R., Jovinge, S., Bloch, W., Bohlen, H., Welz, A., Hescheler, J., Jacobsen, S.E., Fleischmann, B.K., 2006. Engraftment of engineered ES cell-derived cardiomyocytes but not BM cells restores contractile function to the infarcted myocardium. J. Exp. Med. 203, 2315–2327.

Kuzmenkin, A., Liang, H., Xu, G., Pfannkuche, K., Eichhorn, H., Fatima, A., Luo, H., Saric, T., Wernig, M., Jaenisch, R., Hescheler, J., 2009. Functional characterization of cardiomyocytes derived from murine induced pluripotent stem cells in vitro. FASEB J. 23, 4168–4180.

Nembo, E.N., Atsamo, A.D., Nguelefack, T.B., Kamanyi, A., Hescheler, J., Nguemo, F., 2015. In vitro chronotropic effects of *Erythrina senegalensis* DC (Fabaceae) aqueous extract on mouse heart slice and pluripotent stem cell-derived cardiomyocytes. J. Ethnopharmacol. 165, 163–172.

Nguyen, D.C., Hookway, T.A., Wu, Q., Jha, R., Preininger, M.K., Chen, X., Easley, C.A., Spearman, P., Deshpande, S.R., Maher, K., Wagner, M.B., McDevitt, T.C., Xu, C., 2014. Microscale generation of cardiospheres promotes robust enrichment of cardiomyocytes derived from human pluripotent stem cells. Stem Cell Rep. 3, 260–268.

Pfannkuche, K., Liang, H., Hannes, T., Xi, J., Fatima, A., Nguemo, F., Matzkies, M., Wernig, M., Jaenisch, R., Pillekamp, F., Halbach, M., Schunkert, H., Saric, T., Hescheler, J., Reppel, M., 2009. Cardiac myocytes derived from murine reprogrammed fibroblasts: intact hormonal regulation, cardiac ion channel expression and development of contractility. Cell. Physiol. Biochem. 24, 73–86.

Ritner, C., Wong, S.S., King, F.W., Mihardja, S.S., Liszewski, W., Erle, D.J., Lee, R.J., Bernstein, H.S., 2011. An engineered cardiac reporter cell line identifies human embryonic stem cell-derived myocardial precursors. PLoS One 6, e16004.

Schroeder, M., Niebruegge, S., Werner, A., Willbold, E., Burg, M., Ruediger, M., Field, L.J., Lehmann, J., Zweigerdt, R., 2005. Differentiation and lineage selection of mouse embryonic stem cells in a stirred bench scale bioreactor with automated process control. Biotechnol. Bioeng. 92, 920–933.

van Laake, L.W., Qian, L., Cheng, P., Huang, Y., Hsiao, E.C., Conklin, B.R., Srivastava, D., 2010. Reporter-based isolation of induced pluripotent stem cell- and embryonic stem cell-derived cardiac progenitors reveals limited gene expression variance. Circ. Res. 107, 340–347.